The Influence of Temperature and Moisture on the Mode I Fracture Toughness and Associated Fracture Morphology of a Highly Toughened Aerospace CFRP

T. J. Katafiasz[1*], E. S. Greenhalgh[1], G. Allegri[2], S. T. Pinho[1], P. Robinson[1]

[1]Department of Aeronautics, Imperial College London, Exhibition Road, London, SW7 2AZ, UK

[2]Bristol Composites Institute (ACCIS), University of Bristol, Queen's Building, Bristol, BS8 1TR, UK

*Corresponding Author Email: tomas.katafiasz11@imperial.ac.uk

Abstract

This paper addresses the characterisation of the mode I interlaminar fracture toughness of a carbon fibre/epoxy composite material, toughened with thermoplastic particles in the ply interlayers. The characterisation is undertaken at -55°C, 19°C, and 90°C, on both dry and fully moisture saturated coupons. Fractographic observations of the delamination surfaces allows identification of the failure mechanisms. The mode I propagation fracture toughness tested at wet/90°C exhibits a 176% increase compared to the dry/19°C specimens, due to enhanced plastic deformation of the interlayers and more prominent fibre bridging. Moisture-saturated coupons tested at -55°C suffered a 57% reduction of mode I fracture toughness compared to those under dry/19°C conditions. This is due to the dis-bond and consequent plucking of the thermoplastic particles from the surrounding matrix. This observation points to the fact that wet/cold

conditions may represent the worst-case scenario for the interlaminar fracture performance of composite systems toughened with thermoplastic interleaves.

Keywords:

Delamination (B); Environmental degradation (B); Toughened interphase; Fractography (D)

1. Introduction

Delamination, often as a consequence of impact damage, has been the principal hinderance to the adoption of composites in primary aerostructures. Delamination resistance, quantified by interlaminar fracture toughness, represents one of the key performance metrics for fibre-reinforced composite materials. Early generation thermoset systems exhibited very low interlaminar toughness values (e.g. G_{IC}=190J/m² for AS4/3501 [1]), and over the last few decades considerable efforts have been made to enhance the delamination resistance of composites. These have recently culminated in systems with homogenously toughened matrices, which yield modest improvements in mode I fracture toughness in excess of 200J/m² [2]. However, fibre-reinforced thermosets comprising discrete toughening particles at ply interfaces (e.g. thermoplastic interleaves) have also been introduced, such as T800/F3900 [3] and T700/M21 [4]. These achieve mode I fracture toughness values of approximately 600J/m² [5] and 1200J/m² [6], respectively. The inclusion of discrete thermoplastic or elastomeric particulates in fibre reinforced epoxy resin composite systems has been documented to improve the mode I fracture toughness by increasing the surface area of interlaminar

cracks by: (i) either localised cavitation in the particle or a the particle/matrix interface, and (ii) plastic shear yielding in the epoxy matrix [7]. Nonetheless, although such systems present very high toughness at room temperature, the effect of the "in-service" environment on delamination, particularly at low and high temperatures combined with moisture, is still poorly understood.

Aerospace components are subjected to a wide spectrum of operating conditions, both in terms of temperature and relative humidity (RH). When an aircraft is held stationary on a runway in a hot/humid climate, temperatures can reach 60°C with 100% RH [8]. During flight at 37000ft cruising altitude, the temperature is usually about -55°C with RH below 30% [9]. Plasticisation due to the presence of moisture can permanently damage composites [10]. This permanent degradation due to moisture has also been noticed to primarily promote damage at the fibre/matrix interface [9-10]. At elevated temperatures the mode I fracture toughness of nominally dry thermoset composite systems increases [12–14], due to a combination of enhanced matrix ductility and fibre bridging. Below 0°C, dry thermoset composites tend to present a reduction in toughness [15][16], attributed to the embrittlement of the matrix. The presence of moisture combined with high temperature further enhances the mode I fracture toughness, since it makes fibre bridging more prominent [17,18]. Under similar environmental conditions, mode II testing produces competing mechanisms whereby the toughness tends to be reduced due to the degradation of fibre/matrix interface, but increased by the plasticisation of the matrix; leading to an overall net gain in toughness [19].

It is therefore important to assess what the effects of these widely variable "in-service" conditions on structural composites are, particularly in terms of interlaminar fracture toughness. In this paper, the investigation is focussed on assessing the effect of temperature and moisture on a state-of-the-art carbon-fibre/epoxy material comprising of ply interleaving with thermoplastic particles. The influence of the environment on the material was experimentally characterised by mode I fracture toughness testing at different temperatures (-55°C, 19°C and 90°C) and moisture content levels (nominally dry and fully saturated). Extensive SEM fractography was carried out to understand how the environment influences the mode I fracture process and how the underlying mechanisms dictate the resulting interlaminar toughness properties.

2. Material, Manufacture, and Conditioning

A thermoplastic interleaved aerospace CFRP, in the form of unidirectional prepreg, was autoclaved according to the manufacturer's recommended curing cycle into laminated plates, each containing 16 plies with 0° orientation. The material system is commercially sensitive. A 60mm long PTFE film was inserted at the mid-plane at one end of the laminated plates, resulting in a nominal laminate thickness of 2.9mm. Double cantilever beam coupons were waterjet cut to 125mm x 20mm in-plane dimensions, with the PTFE insert extending 50mm from one end of each specimen. The specimens were C-scanned to check for eventual manufacturing defects. The specimens were kept in an oven at 40°C for 1 week prior to testing to ensure complete release of moisture. Half of the specimens were then transferred to a Binder KMF 115 102 litre environmental conditioning oven and kept at 70°C/85%RH until they reached

saturation. Travellers accompanying these coupons were periodically weighed according to the ASTM D5229 standard [20], until the specimens moisture uptake had plateaued, which took approximately 272 days. The coupons that underwent the moisture saturation will henceforth be denoted as 'wet', and the others will be indicated as 'dry'. The moisture content of the wet specimens was 0.92 %wt.

Having reached saturation, the wet specimens were wrapped in flash tape except for a region 18mm from the end of the PTFE insert. They were then placed in a drying oven at 40°C for 3 hours, so that the exposed (i.e. un-taped) surface could dry. End-blocks with dimensions 18mm x 20mm x 12mm were bonded to the specimens using Araldite 2011 2-part epoxy adhesive and allowed to cure overnight at room temperature. The flash tape from the wet specimens was removed and further flash tape was applied to the regions between the end-block and the specimen, to prevent moisture-induced degradation of the adhesive bond. The specimens were then placed back into the conditioning oven for a further fourteen days prior to testing, to allow for absorption of any moisture lost from the surface plies during the application of the end-blocks.

3. Mechanical Testing

The ASTM D5528 standard [21], describing the interlaminar fracture toughness characterisation protocol based on DCB coupons, was followed for testing all of the specimens in mode I, performing three repetitions at each condition, i.e. -55°C, 19°C and 90°C temperature (hereafter referred to as cold, room temperature (RT), and hot), dry and wet. It should be noted that an end-block debonded prematurely during the

testing of one specimen (at wet/90°C) and thus two data sets were captured for this condition. Each specimen was painted along one side using a non-xylene based white tip pen. A 0.1mm tip black permanent marker was then used to draw a millimetre scale from the centre of the end block to the end of the specimen on top of the white paint. A 50kN Instron 5969 test machine and Instron environmental chamber were used for all the tests, employing liquid nitrogen to control the temperature in the cold tests.

An Imetrum optical measurement system [22] was used to track the locations of the loading pins and negate the effect of any compliance in the fixture fittings on the displacement reading. This optical measurement was calibrated against the scale on the specimen for monitoring the crack growth. The change in perspective between the tracked ends of the loading pins and the scale drawn on the specimens was considered negligible (at approx. 10mm) given the distance of the camera from the set-up (at approx. 80cm). The specimens were loaded at a stroke rate of 5mm/min and the load signal was captured directly from the 50kN Instron 5969 test machine into the Imetrum optical measurement system using an analog-to-digital converter. The load traces were stored directly into the same data file as the optical measurement data, thus correlating the Instron crosshead load, the optically calibrated displacement, and time. The corresponding video was captured at 10Hz and overlaid with the load, displacement, and time, allowing for efficient post-processing of the crack length. All the specimens were pre-cracked under mode I at a displacement rate of 5mm/min to approximately 54mm delamination length.

4. Data Reduction

The data reduction followed the modified beam theory methodology, outlined in ASTM D5528 [21]. This methodology entails plotting the cubed root of the compliance at each data point versus the crack length. The non-zero slope condition and other effects leading to deviations from elementary beam theory are accounted for using the modified beam theory methodology. Due to the commercially sensitive nature of the material data, all fracture toughness values have been normalised to the dry/room temperature propagation toughness value. This still enables the main purpose of this paper, i.e. to quantify the relative change in toughness. The initiation fracture toughness was taken using the visual onset criteria (VIS), as specified in ASTM D5528 [21]. It should be noted that the initiation toughness is taken as the first data point for each specimen only if all subsequent values are larger, and the remaining data points are averaged to give the propagation value. If any of the propagation toughness values were below the initiation toughness for a given specimen, an initiation toughness was not specified [21]. All data points during the steady-state propagation region of the R-curve were averaged to produce a single propagation toughness value.

SEM (scanning electron microscope) micrography was carried out on the fracture surfaces of the coupons using a Hitachi S-3700N and a LEO Gemini 1525 FEGSEM (field emission gun scanning electron microscope). The FEGSEM was used to provide higher fidelity images of the detail in the fracture morphology and to clarify any observations made using the lower powered Hitachi SEM. The specimens were mounted on to aluminium stubs using Araldite 2011 2-part epoxy, mixed with carbon black to mitigate for specimen charging and allowed to dry overnight. The coupons

were then coated using gold sputtering under vacuum for a total of 20 seconds each. For the FEGSEM imaging, specimens of the fractured surfaces were cut to 10mm x 10mm and mounted on to aluminium stubs using the same epoxy/carbon black mixture described above. The specimens were coated using a 15nm thick Chromium sputtering device under vacuum and were dried fully for 48 hours in a 40°C oven to prevent the expulsion of volatiles under the high vacuum FEGSEM.

5. Results

Figure 1 presents the mode I averaged steady-state propagation toughness versus test temperatures and moisture content, and the graphs in Figure 2 and Figure 3 show the corresponding toughness values versus crack length for the three testing temperatures considered, in both the dry and wet conditions. The wet/hot condition presented an *R*-curve behaviour, whereas the other test conditions were insensitive to crack length. Table 1 presents the normalised initiation and propagation toughness data for each condition, with all the data having been normalised with respect to the dry/RT propagation toughness, hereafter referred to as G_{IC0}. The sparsity of data points for the cold tests was due to the slip-stick nature of the crack propagation at -55°C, leading to fewer stable crack lengths having been recorded during testing.

The dry propagation toughness values presented a negligible variation between the dry/cold and dry/RT tests, and a 37% increase from dry/RT at dry/hot. The wet toughness values exhibited a stronger dependence on temperature than the dry ones, with a 57% drop in toughness in wet/cold conditions, and a 176% increase in toughness

in wet/hot testing, compared to the reference dry/room temperature toughness. The highest toughness was therefore associated with the wet/hot condition, and the lowest was attained in the wet/cold scenario.

Table 1: Normalised initiation and propagation mode I fracture toughness G_{IC} (normalised) (CV%)

	-55°C		19°C	90°C	
	Initiation	**Propagation**	**Propagation**	**Initiation**	**Propagation**
Dry	0.91 (27%)	1.00 (11%)	G_{IC0} = 1.00 (3%)	1.34 (8%)	1.37 (6%)
Wet	0.39 (47%)	0.43 (27%)	0.99 (3%)	-	2.76 (2%)

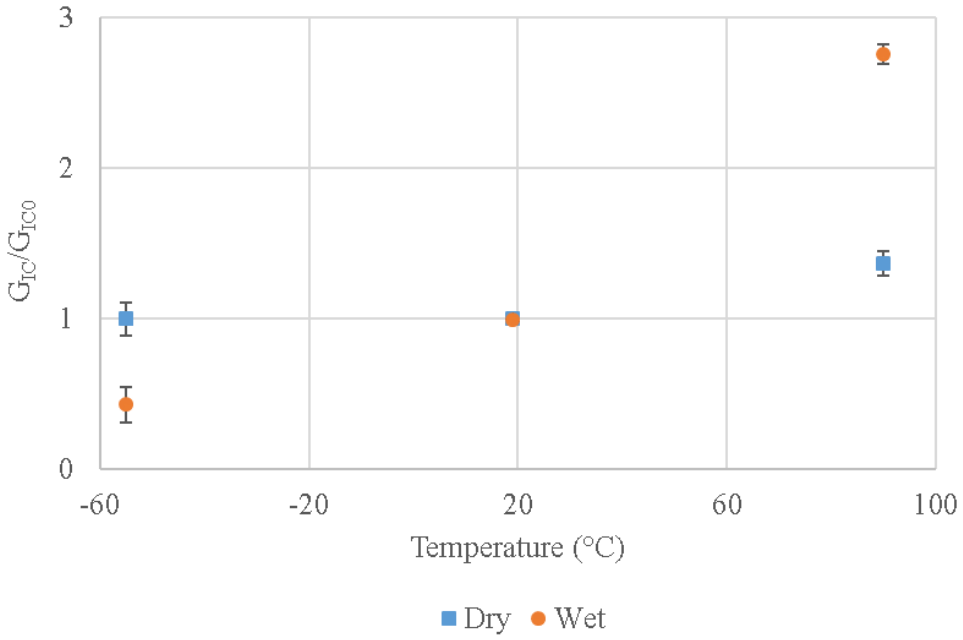

Figure 1. Normalised mode I fracture toughness (G_{IC}/G_{IC0}) versus temperature (°C)

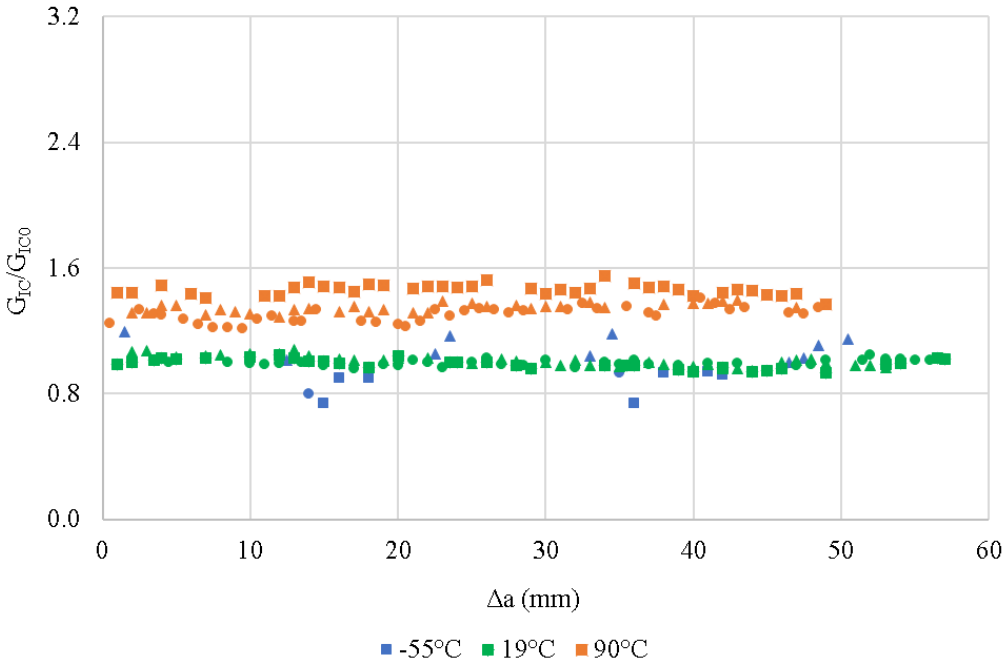

Figure 2. Normalised mode I fracture toughness (G_{IC}/G_{IC0}) versus change in crack length (mm) for the dry specimens

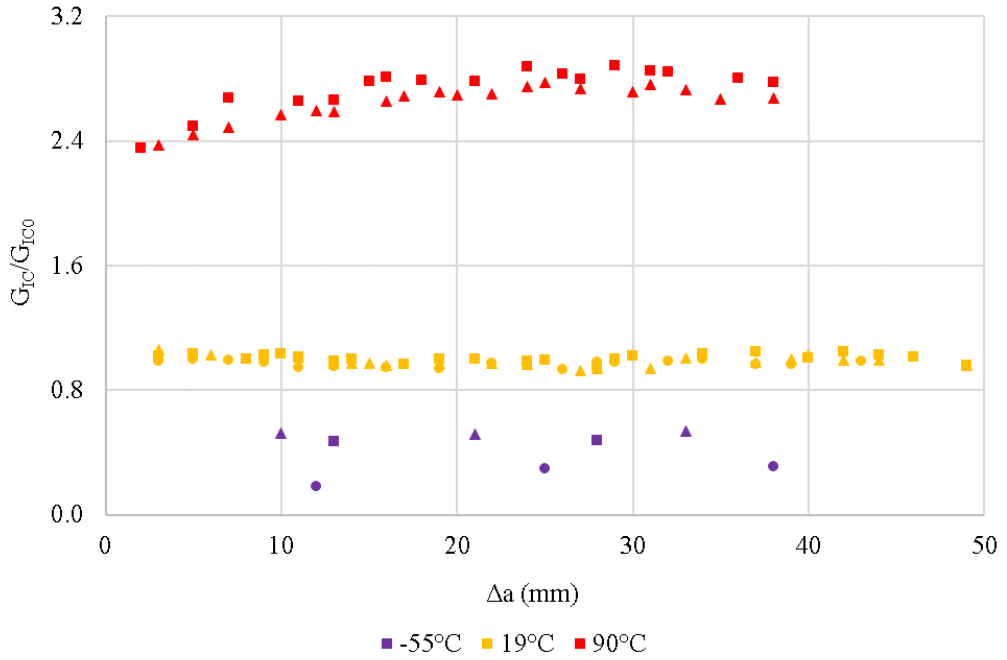

Figure 3. Normalised mode I fracture toughness (G_{IC}/G_{IC0}) versus change in crack length (mm) for the wet specimens

6. Fractography

The fractography provided an insight in the damage processes which ensued during progressive delamination. The micrographs in the Figures that follow in this section were taken from the propagation region of the mode I fracture, at a crack length of approximately 30mm from the crack initiation site. The crack growth direction in each image is from the top towards the bottom and is representative of the morphology present within the propagation region of each interlaminar fracture.

Figure 4 presents the fracture surface morphology at 200x magnification. Uniformly distributed toughened particles approximately 20μm in diameter and not to be confused with the darker voids within each particle, were visible in all coupons tested, independent from the temperature. These particles are indeed characteristic of the interlaminar toughened phase, as confirmed by the observation of polished sections of the material before testing.

Each particle contained one or two internal voids (small, dark circular features) which were present prior to the interlaminar fracture of the composite. The majority of the fracture was cohesive, i.e. midplane within the resin-rich interlayer, but some interfacial fibre/matrix failure was noted, particularly in the wet/RT and wet/hot conditions. The dry/RT surface presented a relatively brittle epoxy fracture, with cleavage of the particles on the same plane as the epoxy. A similar morphology was noticed in the dry/cold regime, showing a smooth epoxy surface, consistent with a high degree of brittle fracture. The dry/hot regime presented a more ductile failure, evident in the higher magnification micrographs in Figure 6 and Figure 7, where the epoxy was seen to have plastically

deformed across the fracture surface. The wet/RT morphology showed a more ductile epoxy fracture compared to that of the dry/RT surface, with presence of fibre/matrix debonding, where fibre imprints were observed. The wet/cold surface exhibited a similar morphology to that of the dry/cold, with brittle fracture of the epoxy and brittle cleavage of the toughening particles. The wet/hot surface presented the largest amount of plastic deformation of the epoxy across all test regimes, with high levels of ductile flow as well as substantial fibre/matrix debonding.

Figure 5, Figure 6, and Figure 7 present the surface morphologies at 500x, 1000x, and 5000x magnification, respectively. The dry/RT surface exhibited low levels of plastic deformation for both the epoxy matrix and the particles. The dry/hot surfaces showed considerable plastic deformation within the toughening particles, with fibrillation extending from their outer surfaces towards the centre of each particle. The wet/RT morphology exhibited high levels of ductility in the epoxy, as well as indications of fibre/matrix interfacial debonding. The wet/cold morphology presented brittle epoxy fracture and cleavage of the toughening particles, with a small amount of plucking of the particles, as illustrated by the step change in fracture plane at 5000x magnification. The wet/hot morphology exhibited extremely high levels of ductile flow across the epoxy and in the toughening particles, along with large areas of fibre/matrix debonding also visible at 200x magnification.

Figure 8 presents the FEGSEM images of the dry/cold and wet/cold specimen fracture morphology. Both test regimes were seen to promote brittle fracture throughout the epoxy resin phase. The dry/cold surfaces presented cleavage across both the epoxy and

the toughening particles, with the internal voids clearly visible where the particles had been cleaved. This observation demonstrates that these were pre-existing voids, and not artefacts of ductile flow of the toughened phase. A faint boundary between the toughened particle and epoxy can be observed in the dry/cold 5000x magnification image. For the wet/cold surface morphology, plucking of the toughening particles was evident, since both smooth particle surfaces and particle imprints in the epoxy were visible. A clear debond between the toughening particle and the surrounding epoxy is apparent in the wet/cold 5000x magnification FEGSEM image in Figure 8, where a step change in the fracture plane was noted.

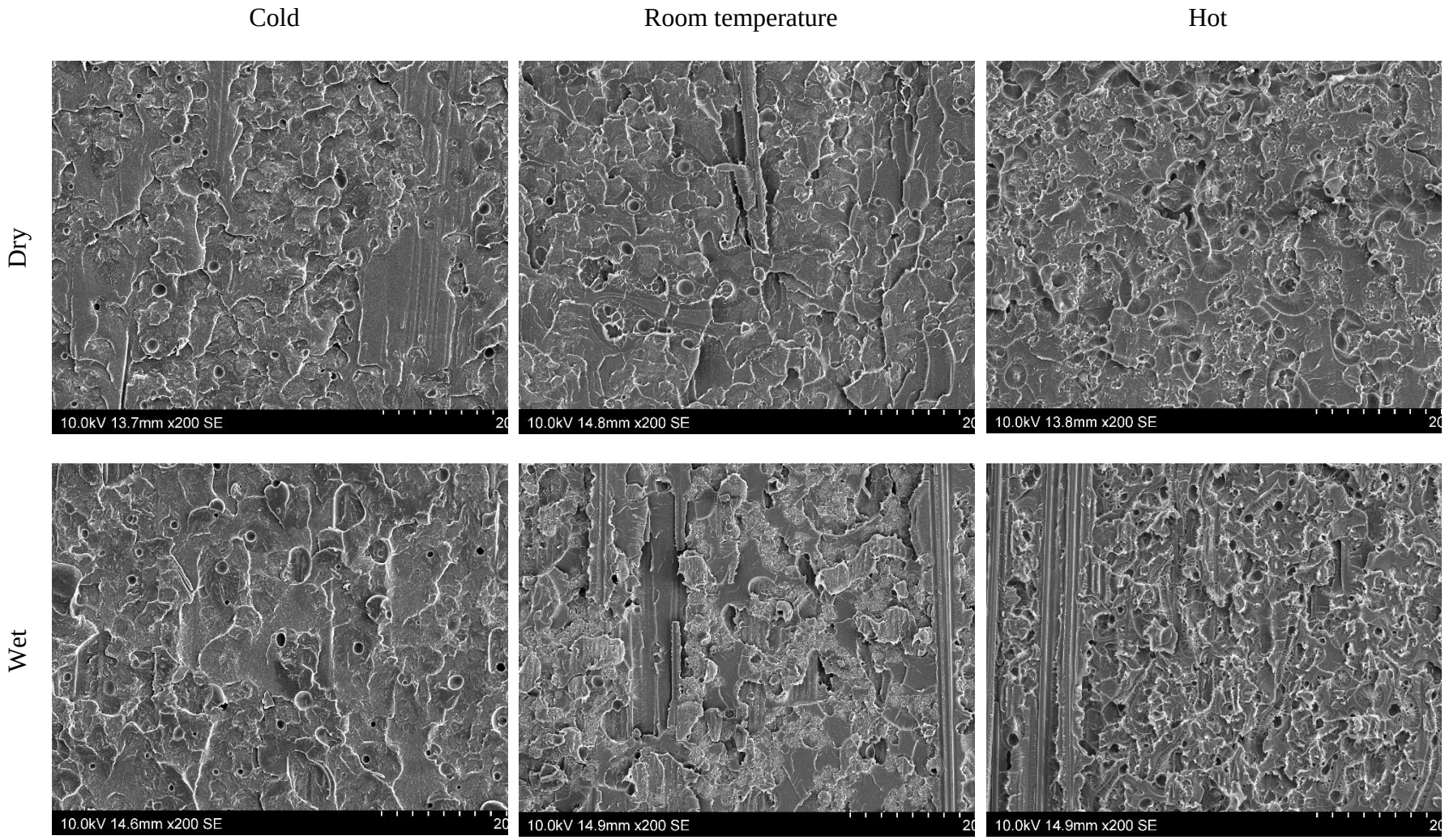

Figure 4. Representative SEM micrographs of the mode I fracture morphology, 200x

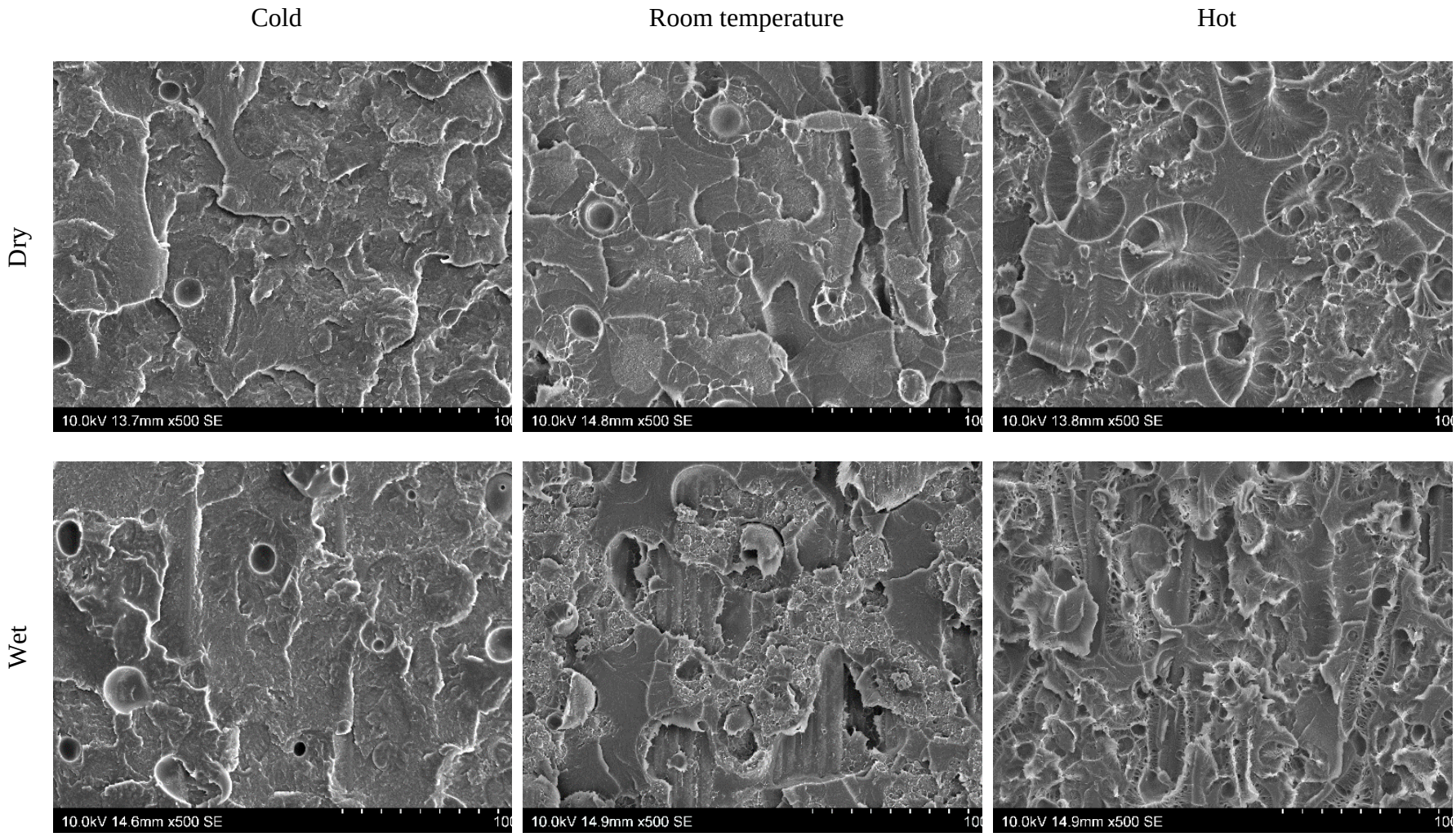

Figure 5. Representative SEM micrographs of the mode I fracture morphology, 500x

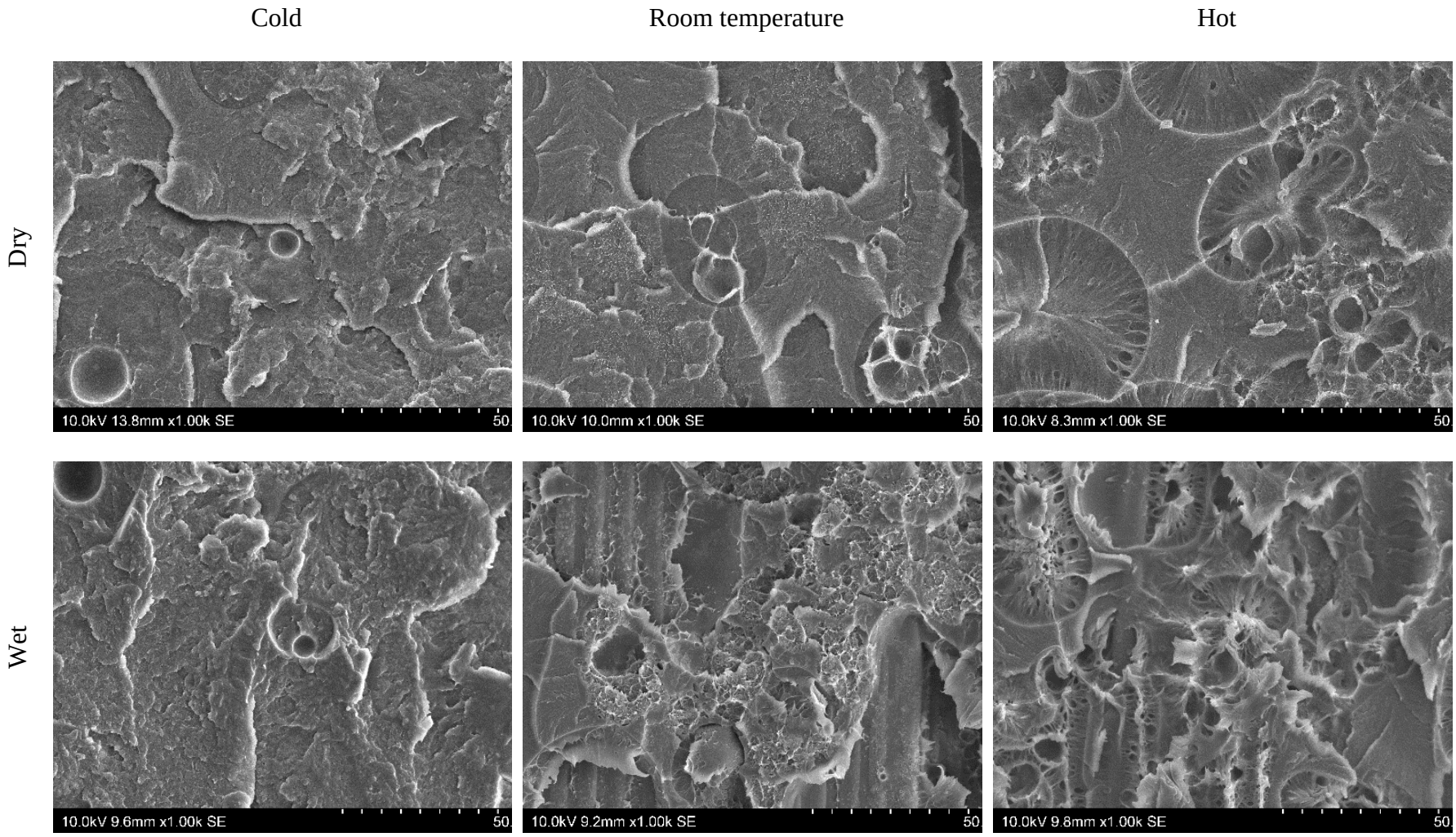

Figure 6. Representative SEM micrographs of the mode I fracture morphology,1000x

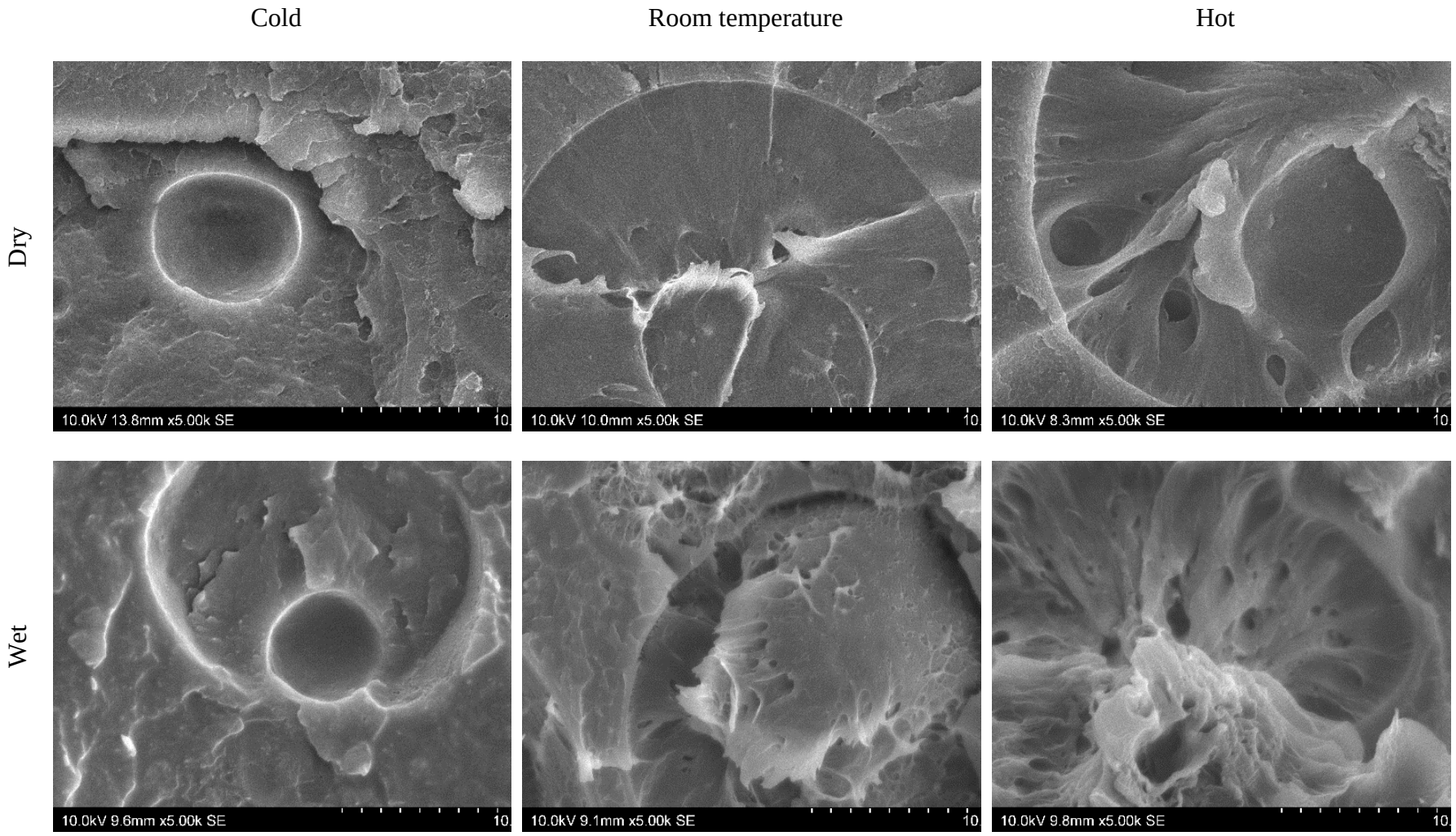

Figure 7. Representative SEM micrographs of the mode I fracture morphology, 5000x

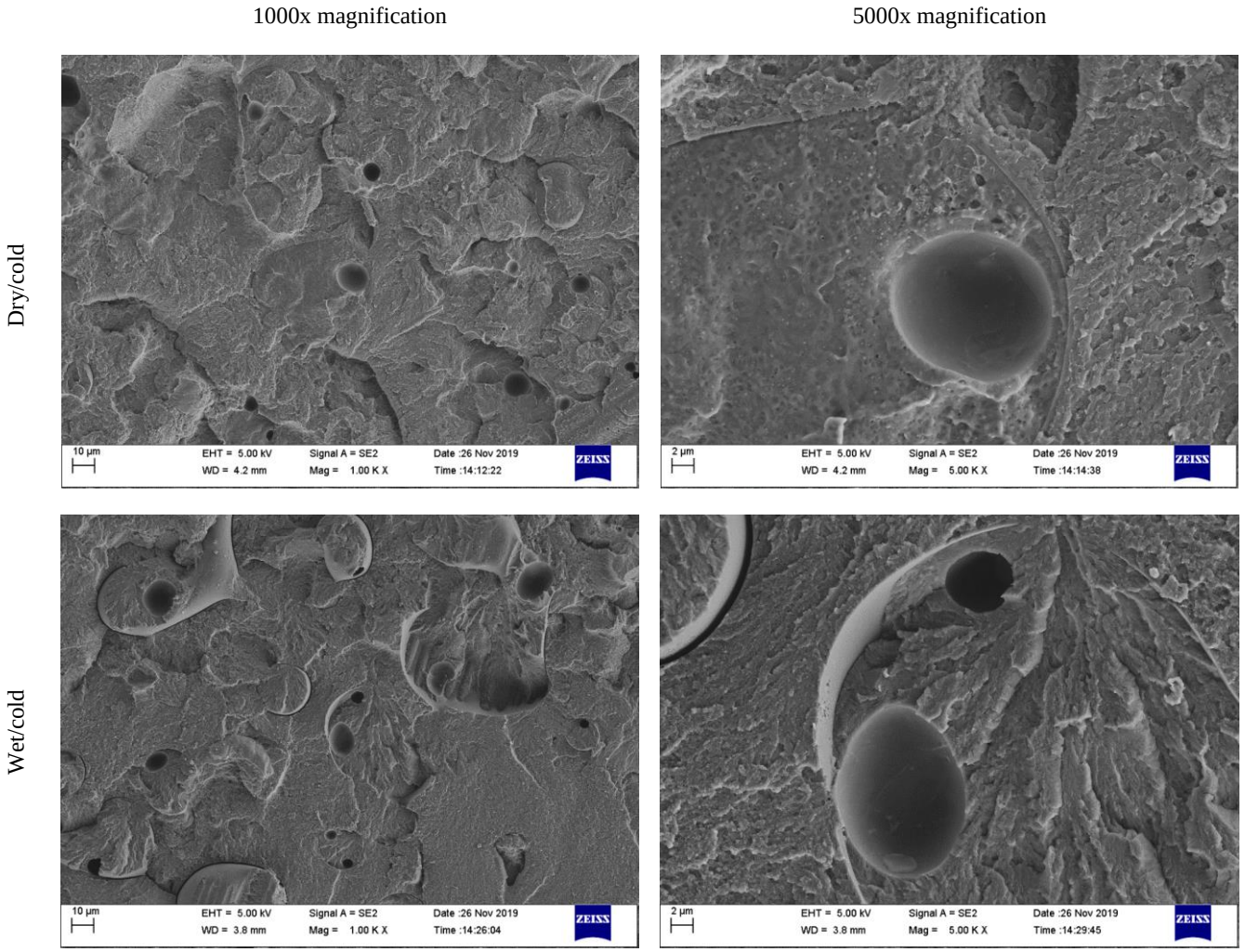

Figure 8. Representative FEGSEM micrographs of the mode I dry/cold and wet/cold fracture morphology, 1000x and 5000x

7. Discussion

The micrographs presented previously clearly demonstrate the role played in the fracture process by the toughening particles dispersed throughout the epoxy matrix. It is worth pointing out again that the dark circular features clearly visible across all specimens are voids within the particles.

The dry/RT surface morphology presented brittle fracture across the epoxy interlayer, with evidence of some ductility within the toughening particles. These features were also observed in the dry/RT SEM image morphologies at 1000x and 5000x magnifications. A similar morphology was recognised in the dry/cold tests, but with a smoother surface within the cleaved toughening particles, indicating a highly brittle fracture. The fracture toughness values for these two conditions (i.e. dry/RT and dry/cold) were almost identical, as it should be expected given the stark similarity of the surface morphologies. The dry/hot surface exhibited void coalescence and a more ductile fracture of both the epoxy and toughening particles, compared to those observed in the dry/RT coupons. There was no evidence of fibre/matrix debonding in the dry/hot condition, but the high levels of ductile flow led to the observed 37% increase in fracture toughness, relative to the dry/RT tests.

The wet/RT morphology presented high levels of ductility across both the epoxy and toughening phases. There was some evidence of toughening particle/epoxy debonding in both the wet/RT and wet/cold surfaces, where steps were visible at the particle/epoxy boundary. The wet/cold morphology presented a highly brittle fracture, and large levels

of plucking of toughening particles. The FEGSEM micrographs further confirmed this observation, since smooth particle surfaces and imprints were visible across the fracture surface. These two mechanisms, i.e. particle/epoxy debonding and subsequent particle plucking, led to a 57% drop in fracture toughness compared to both the dry/RT and dry/cold tests.

The wet/hot morphologies presented the highest levels of ductile flow across both the epoxy and toughening particles. High levels of fibre/matrix debonding were noted in this regime, leading to a highly ductile and tortuous crack path, and hence a substantial 176% increase in fracture toughness, compared to the dry/RT tests. It is evident that the toughening particle/epoxy interface was weakened by the moisture conditioning prior to testing. However, the eventual dis-bond between the particles and the surrounding matrix was not visible following testing in wet/hot conditions, due to the substantial plastic deformation affecting of the phases in the ply interlayer. The degradation of the fibre/matrix interface in the wet/hot tests explains the observed rise in the toughness with crack length (Figure 3).

It should be noted that there were competing failure mechanisms evident in the wet coupons. Although the wet/RT fracture toughness was almost identical to that of the dry/RT tests, the corresponding failure morphologies were very different. The wet/RT specimens exhibited some plucking of toughening particles, inherently a low-energy process and likely leading to a net reduction in toughness. However, the degradation of the fibre/matrix interface in the wet/RT condition likely counteracted this apparent reduction in toughness due to particle plucking, by promoting a more tortuous crack

path and therefore plastic deformation of the epoxy, resulting in an overall fracture toughness similar to that of the dry/RT condition. The 57% decrease in the wet/cold fracture toughness was due to the toughening particle/epoxy debonding and particle cleavage. The 176% increase in fracture toughness in the wet/hot condition was due to the high ductility displayed both by the particles and the surrounding epoxy. Moreover, the degradation of the fibre/matrix interface led to a torturous crack path and a rising *R*-curve due to fibre bridging. It should be noted however that the increase in fibre bridging under the wet/hot condition is an implication of the relative weakening of the fibre/matrix interface. This increase in fracture toughness was noticed regardless of the degradation of the particle/epoxy interface due to the moisture, although not explicitly visible in the fractography due to the large amount of plastic flow that had occurred. Overall, the stark difference in mode I fracture toughness between dry and wet coupons at -55°C suggests that the dis-bond of the thermoplastic particles from the surrounding epoxy matrix is triggered by the mismatch in coefficients of moisture expansion of the two phases within the ply interlayers.

8. Conclusions

The objective of this research was to characterise the relative changes in mode I interlaminar toughness for interleaved toughened epoxy systems in aerospace composite structures under realistic environmental conditions. Since aerospace structures are exposed to a wide range of humidity and temperature conditions during service, it is imperative that the material properties are assessed in these conditions. This study has focussed on the mode I interlaminar fracture toughness, complementing ASTM-

standard testing with detailed fractographic observations. The key conclusions drawn from the work undertaken are the following:

- In dry/room temperature conditions, the epoxy matrix fractured in a brittle fashion, with the toughening particles exhibiting some level of ductility. The dry/cold tests showed a more brittle surface morphology, but with an almost identical fracture toughness. In the dry/hot tests high levels of ductility were observed in all the phases within the ply interlayers, leading to a 37% fracture toughness increase compared to dry/room temperature tests.
- Debonding between the thermoplastic particles and the surrounding matrix occurred prior to testing both in the wet/room temperature and wet/cold tests. A 57% reduction in toughness for the wet/cold tests was attributed to the highly brittle fracture of the epoxy phase and plucking of the toughening particles. The latter essentially prevents any beneficial influence of the particles on the fracture toughness.
- The substantial 176% increase of fracture toughness observed in the wet/hot tests compared to dry/room temperature conditions was due to the high levels of ductility in both the epoxy and toughening particles. The weakening of the fibre/matrix interface due to the moisture led to enhanced fibre bridging during crack propagation resulting in a non-linear *R*-curve for the hot/wet condition. Regardless of this fibre bridging, the fractography conducted provides morphological evidence of a reduction in toughness at lower temperatures, with brittle fracture of the toughened phase at -55°C.
- It is evident that the interleaved toughened system characterised in this study presents excellent properties in wet/hot conditions, which are traditionally

considered the most critical for aerostructures. However, under wet/cold conditions, these highly toughened systems present a considerable drop in toughness compared to the dry/room temperature reference state. The cause of this drop is the degradation of the interface between the toughened particles and epoxy phases, which is likely to occur because of the mismatch in coefficients of moisture expansion.

- Due to the relatively thick interleave, fibre nesting at the 0°/0° interface in the material tested was not as prominent as in conventional composites. It is therefore anticipated that additional mechanisms at non-zero ply interface failures [23], often noticed in-service failures, will not be as prominent. Therefore, the critical observation that the toughened phase is more brittle and undergoes plucking at lower temperatures will be common across non-zero interfaces as well. Moreover, mode I (DCB) testing is widely used to assess the toughness of a matrix system, whereas mode II tests are dominated more by the fibre/matrix interfacial strength. Therefore, the experimental evidence and the observation of the failure surface morphologies suggest that fibre-reinforced epoxy systems toughened with thermoplastic particles may be more susceptible to fracture in wet/cold conditions than in wet/hot scenarios under mode I dominated conditions. This behaviour should be properly accounted for in the design process of aerospace components.

Acknowledgements

Funding from Innovate UK, ATI and Rolls-Royce plc via the collaborative research projects ‘CTI Composite Fan Technology’ [grant number 113085] and ‘FANTASTICAL’ [grant number 113190] is gratefully acknowledged. Manufacturing assistance from Mr Jonathan Cole and Mr Gary Senior, and testing assistance from Mr Keith Wolstenholme and Mr Joseph Meggyesi is also acknowledged.

References

[1] W. Johnson, P. Mangalgiri, Influence of the Resin on Interlaminar Mixed-Mode Fracture, Toughened Composites. ASTM STP 9 (1987) 295–315. https://doi.org/10.1520/stp24384s.

[2] M.W. Czabaj, J.G. Ratcliffe, Comparison of intralaminar and interlaminar mode I fracture toughnesses of a unidirectional IM7/8552 carbon/epoxy composite, Composites Science and Technology. 89 (2013) 15–23. https://doi.org/10.1016/j.compscitech.2013.09.008.

[3] M.B. Dow, D.L. Smith, Properties of Three Graphite/Toughened Resin Composites: NASA-TP-3102, Hampton, Virginia, 1991.

[4] Hexcel, HexPly ® M21 - Product Data Sheet - EU Version, Hexcel. (2015) 1–6. https://doi.org/FTA-002-AG16.

[5] N. Encinas, B.R. Oakley, M.A. Belcher, K.Y. Blohowiak, R.G. Dillingham, J. Abenojar, M.A. Martínez, Surface modification of aircraft used composites for adhesive bonding, International Journal of Adhesion and Adhesives. 50 (2014)

157–163. https://doi.org/10.1016/j.ijadhadh.2014.01.004.

[6] D.N. Markatos, K.I. Tserpes, E. Rau, S. Markus, B. Ehrhart, S. Pantelakis, The effects of manufacturing-induced and in-service related bonding quality reduction on the mode-I fracture toughness of composite bonded joints for aeronautical use, Composites Part B: Engineering. 45 (2013) 556–564. https://doi.org/10.1016/j.compositesb.2012.05.052.

[7] A.C. Garg, Y.W. Mai, Failure mechanisms in toughened epoxy resins-A review, Composites Science and Technology. 31 (1988) 179–223. https://doi.org/10.1016/0266-3538(88)90009-7.

[8] E.D. Coffel, T.R. Thompson, R.M. Horton, The impacts of rising temperatures on aircraft takeoff performance, Climatic Change. 144 (2017) 381–388. https://doi.org/10.1007/s10584-017-2018-9.

[9] International Civil Aviation Organization, Manual of the ICAO Standard Atmosphere (extended to 80 kilometres (262 500 feet)) (Third ed.) ISBN: 92-9194-004-6, (1993).

[10] K. Friedrich, Application of Fracture Mechanics to Composite Materials, Elsevier, 1987.

[11] Kishore, A. Maiti, Compressive behavior and fracture features of rubber bearing glass-epoxy composites exposed to aqueous media, Journal of Reinforced Plastics and Composites. 20 (2001) 1546–1554. https://doi.org/10.1106/92BG-4C2Q-DBN7-LL4G.

[12] D. Hunston, R. Moulton, N. Johnston, W. Bascom, Matrix Resin Effects in Composite Delamination: Mode I Fracture Aspects, Toughened Composites.

(2008) 74-74–21. https://doi.org/10.1520/stp24372s.

[13] K.D. Cowley, P.W.R. Beaumont, The interlaminar and intralaminar fracture toughness of carbon-fibre/polymer composites: The effect of temperature, Composites Science and Technology. 57 (1997) 1433–1444. https://doi.org/10.1016/S0266-3538(97)00047-X.

[14] A. Watt, A.A. Goodwin, A.P. Mouritz, Thermal degradation of the mode I interlaminar fracture properties of stitched glass fibre/vinyl ester composites, Journal of Materials Science. 33 (1998) 2629–2638. https://doi.org/10.1023/A:1004365521648.

[15] J.J.M. Machado, E.A.S. Marques, R.D.S.G. Campilho, L.F.M. da Silva, Mode I fracture toughness of CFRP as a function of temperature and strain rate, Journal of Composite Materials. 51 (2017) 3315–3326. https://doi.org/10.1177/0021998316682309.

[16] M.S. Oliver, W.S. Johnson, Effect of temperature on mode i interlaminar fracture of IM7/PETI-5 and IM7/977-2 laminates, Journal of Composite Materials. 43 (2009) 1213–1219. https://doi.org/10.1177/0021998308104147.

[17] B.D. Davidson, M. Kumar, M.A. Soffa, Influence of mode ratio and hygrothermal condition on the delamination toughness of a thermoplastic particulate interlayered carbon/epoxy composite, Composites Part A: Applied Science and Manufacturing. 40 (2009) 67–79. https://doi.org/10.1016/j.compositesa.2008.10.006.

[18] R. Olsson, Factors Influencing the Interlaminar Fracture Toughness and Its Evaluation in Composites, (1991) 34 FFA TN.

[19] M. Todo, T. Nakamura, K. Takahashi, Effects of Moisture Absorption on the Dynamic Interlaminar Fracture Toughness of Carbon/Epoxy Composites, Journal of Composite Materials. 34 (2000) 630–648.

[20] ASTM standard, - ASTM D 5229– 92 – Standard Test Method for Moisture Absorption Properties and Equilibrium Conditioning of Polymer Matrix Composite Materials, ASTM Standard. 92 (2010) 1–13. https://doi.org/10.1520/D5229.

[21] ASTM Int'l, ASTM D5528: Standard Test Method for Mode I Interlaminar Fracture Toughness of Unidirectional Fiber-Reinforced Polymer Matrix Composites, American Standard of Testing Methods. 03 (2014) 1–12. https://doi.org/10.1520/D5528-13.2.

[22] Imetrum Ltd., Imetrum Precision Displacement Trackers, (2020). https://www.imetrum.com/products/precision-displacement-trackers/ (accessed January 31, 2020).

[23] E.S. Greenhalgh, Failure analysis and fractography of polymer composites, 2009. https://doi.org/10.1533/9781845696818.164.